

ELASTIC-PLASTIC MODELS FOR MULTI-SITE DAMAGE ¹

Ricardo L. Actis
Engineering Software Research and Development, Inc.
St. Louis, MO

S₁-39
23095
p. 16

Barna A. Szabó
Center for Computational Mechanics
Washington University, St. Louis, MO

SUMMARY

This paper presents recent developments in advanced analysis methods for the computation of stress intensity factors and the J-integral under conditions of small scale yielding in structural panels with multi-site damage. The method of solution is based on the p-version of the finite element method. Its implementation was designed to permit extraction of linear stress intensity factors using a superconvergent extraction method (known as the contour integral method) and evaluation of the J-integral following an elastic-plastic analysis. Coarse meshes are adequate for obtaining accurate results supported by p-convergence data. The elastic-plastic analysis is based on the deformation theory of plasticity and the von Mises yield criterion.

The model problem consists of an aluminum plate with six equally spaced holes and a crack emanating from each hole. The cracks are of different sizes. The panel is subjected to a remote tensile load. Experimental results are available for the panel. The plasticity analysis provided the same limit load as the experimentally determined load. The results of elastic-plastic analysis were compared with the results of linear elastic analysis in an effort to evaluate how plastic zone sizes influence the crack growth rates. The onset of net-section yielding was determined also. The results show that crack growth rate is accelerated by the presence of adjacent damage, and the critical crack size is shorter when the effects of plasticity are taken into consideration. This work also addresses the effects of alternative stress-strain laws: The elastic-ideally-plastic material model is compared against the Ramberg-Osgood model.

INTRODUCTION

Reliable stress intensity factor computation of cracked structural components is of major importance in modern design of aircraft structures where requirements for residual strength and fatigue crack propagation must be met. In this paper the problem of computing the stress intensity factors for a structural panel with multi-site damage, with guarantee of reliability, is discussed. This work focuses on the accuracy and reliability of the numerical solution of a proposed mathematical model and on the influence that different modeling assumptions may have on the results of the analysis. Two kinds of error are important in this case:

1. The differences between the exact solution of the mathematical problem formulated to represent a physical system or process and its numerical approximation are called errors of discretization. Is it possible to guarantee that the error of discretization is small?

1. Work supported by NASA Lyndon B. Johnson Space Center under Grant NAG 9-622.

2. The differences between the exact solution of the mathematical problem formulated to represent a physical system and the actual response or behavior of the physical system are called errors of idealization or modeling errors. How does incorporating plasticity in the analysis affect the stress intensity factors?

In some cases the two errors, the errors of discretization and modeling, may partially cancel one another. Therefore it is important to verify by means other than the experiment itself, that the numerical solution is close to the exact solution of the model. Only then is it possible to investigate whether the errors of idealization are large or small by making comparisons with experimental observations. The efficient and reliable control of numerical errors, achieved by the use of a superconvergent method for the computation of the stress intensity factors, makes it feasible to investigate the sensitivity of crack extension to alternative modeling decisions.

In this paper, the effect of plasticity on the values of the fracture mechanics parameters is investigated. First, the finite element implementation is discussed; and second the method is illustrated with the integrity assessment of a row of fastener holes with multi-site damage, for which experimental results are available.

FINITE ELEMENT IMPLEMENTATION

Choice of an Extension Process

In the finite element method the control of the errors of discretization can be achieved by mesh refinement (h-extension), by increasing the polynomial degree of elements (p-extension), or a combination of both (hp-extension).

The size of a finite element is the diameter of the smallest circle (or sphere) that contains the element. This diameter is denoted by h and the diameter of the largest finite element in the mesh is denoted by h_{max} . h-Extension involves letting $h_{max} \rightarrow 0$. Alternatively, we can hold the number of elements constant and increase the polynomial degree of elements. The polynomial degree of elements is a vector p . p-Extension involves letting the smallest polynomial degree $p_{min} \rightarrow \infty$. In hp-extensions mesh refinement is combined with an increase of the polynomial degree of elements. In these processes the number of equations that has to be solved, the number of degrees of freedom, is progressively increased, hence the name 'extension'. Note that h- and p-extensions can be viewed as special cases of hp-extension, which is the general discretization strategy of the finite element method.

An important question is: "Which is the most efficient method of extension with respect to reducing discretization errors?" This question can be answered on the basis of a simple classification of the exact solution of the problem one wishes to solve. The exact solutions (u_{EX}) have been classified into three main categories:

Category A: u_{EX} is analytic. A function is analytic at a point if it can be expanded into a Taylor series about that point on the entire solution domain, including the boundaries of the solution domain. Alternatively, the domain can be divided into subdomains and u_{EX} is analytic on each subdomain, including the boundary of each subdomain. The finite element mesh is so constructed that the boundaries of the subdomains are coincident with element boundaries.

Category B: u_{EX} is analytic on the entire domain, including the boundaries, with the exception of a finite number of points (in three dimensions u_{EX} needs not be analytic along a finite number of lines). The mesh is so constructed that the points where u_{EX} is not analytic are nodal points (in three dimensions the

lines where u_{EX} is not analytic are coincident with element edges). An example of problems in Category B is a cracked elastic body. The crack tip is a singular point.

Category C: Problems for which the exact solution is neither in Category A nor in Category B are in Category C.

Most problems in mechanical and structural design belong in either Category A or Category B. Most problems in fluid dynamics belong in Category C. Knowing the classification of a problem, it is possible to compare h-, p- and hp-extensions on the basis of rate of convergence, that is, the rate of change of the error measured in energy norm with respect to the number of degrees of freedom. For problems in Category A and B the discretization errors are most efficiently controlled by p-extension. Designing a mesh such that when the polynomial degree of elements is uniformly increased then the discretization error decreases exponentially until the required degree of accuracy has been reached; usually it involves grading the mesh in geometric progression in the vicinity of singular points (ref. 1).

The Trunk and Product Spaces

By definition, the standard quadrilateral element $\Omega_{st}^{(q)}$ is the set of points (ξ, η) which satisfy $|\xi| \leq 1$, $|\eta| \leq 1$, see Figure 1. The *trunk space* of degree p is defined as the set of polynomials which can be

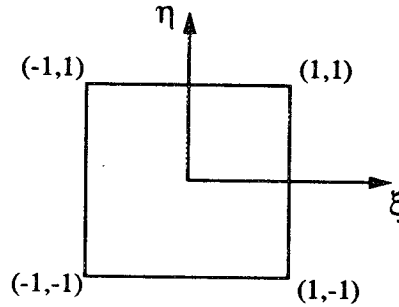


Figure 1. The standard quadrilateral element $\Omega_{st}^{(q)}$.

expressed as linear combinations of $\xi^i \eta^j$, $i, j = 0, 1, \dots, p$; $i + j \leq p$ and supplemented by the monomial term $\xi \eta$ for $p=1$, and the monomial terms $\xi^p \eta$, $\xi \eta^p$ for $p \geq 2$. For example, for $p=4$ the trunk space includes all polynomials up to degree 4, plus two fifth order polynomials. The *product space* of degree p is the set of polynomials which can be expressed as linear combinations of $\xi^i \eta^j$, $i, j = 0, 1, \dots, p$. For example, for $p=4$ the product space includes all polynomials up to degree 8.

The answer to the question: "Which space should be used in a given application?" depends on the accuracy requirements. The following points should be taken into consideration:

1. The number of degrees of freedom increases much more rapidly with respect to p when the product space is used. For example, in the case of $p=8$ there are 47 degrees of freedom per field for the trunk space, and 81 degrees of freedom per field for the product space.
2. For a given polynomial degree the error, measured in energy norm, is always smaller for the product space than for the trunk space. This is because the trunk space is a subset of the product space.
3. For a given number of degrees of freedom the error for the product space, measured in energy norm, may be smaller or larger than the error for the trunk space. There appears to be no way of predicting which space performs better for specific cases.

4. For static analyses, work performed by the computer increases more slowly with respect to increasing p for the product space than for the trunk space. This is because in the case of the product space the increase affects the internal modes only and those modes are eliminated by the solver locally, i.e. no assembly is involved and the front width is unaffected.

In our implementation both the trunk and product spaces are available for quadrilateral elements, and the polynomial degree can be increased up to $p=8$.

Elastic-Plastic Analysis

The implementation of material nonlinearities within the framework of the p -version was considered an essential feature in the assessment of modeling assumptions. The elastic-plastic analysis is based on the von Mises yield criterion and the deformation theory of plasticity. The purpose and scope of this implementation are as follows (for further details see ref. 2):

1. Realistic mathematical models of real physical systems must have a capability to provide initial estimates for the effects of nonlinearities at a low computational cost. The deformation theory of plasticity serves this purpose well for a large class of practical problems.
2. The effects of a single overload event on structures made of ductile materials are of substantial practical importance. Such effects can be well represented by mathematical models based on the deformation theory of plasticity, provided that the plastic flow is contained, i.e., the plastic zone is surrounded by elastic material.
3. The propagation of cracks in strain-hardening materials is generally correlated with the J-integral. The J-integral is based on the deformation theory of plasticity.
4. An important feature of the linear implementation is that engineering data can be conveniently extracted from finite element solutions in the post-solution phase. The deformation theory of plasticity makes it feasible to extend this into the elastic-plastic regime because the data storage requirements are small.
5. The p -version is not susceptible to Poisson ratio locking and hence correct limit loads are obtained. In the conventional (h -version) locking occurs when the displacement formulation is used. For this reason alternative formulations, generally known as mixed methods, must be employed.

Elastic-Plastic Material Properties

An important modeling assumption is the type of stress-strain law used for the elastic-plastic analysis. Four types of stress-strain relationships have been implemented:

Ramberg-Osgood: Material characterized by four parameters (Figure 2): The modulus of elasticity (E), Poisson's ratio (ν), the stress (S_{70E}), which is the stress corresponding to the intersection of the stress-strain curve with a line which passes through the origin and has the slope of $0.70E$, and an exponent n in the expression:

$$\epsilon = \frac{\sigma}{E} + \frac{S_{70E}}{E} \left(\frac{\sigma}{S_{70E}} \right)^n \quad (1)$$

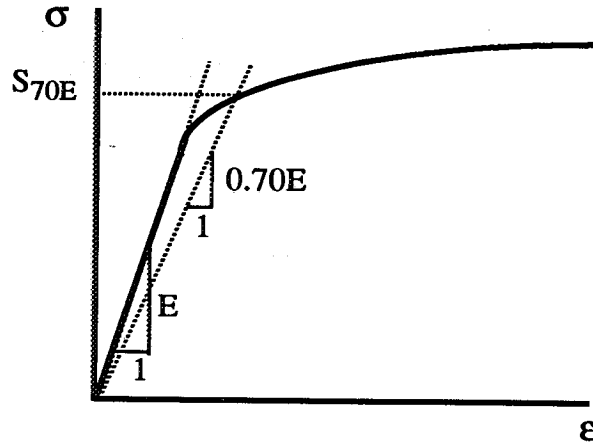


Figure 2. The Ramberg-Osgood stress-strain curve.

Typical values of n range between 4 and 90. Fractional values are permitted for n . In the limit as $n \rightarrow \infty$, an elastic-perfectly plastic material behavior is approached.

Elastoplastic: Elastic-perfectly plastic material characterized by E , ν and the yield stress S_y .

Bilinear: Linear-elastic, linear strain hardening material characterized by E , ν , S_y and the tangent modulus E_t which characterizes strain hardening.

5-Parameter: Material characterized by two linear segments joined by a cubic spline.

Solution Algorithm

The following is an outline of the solution procedure implemented for two-dimensional elastic-plastic problems based on the deformation theory of plasticity. The procedure is known as direct integration. The iteration number is represented by a superscript in brackets:

1. Obtain a linear solution for the problem. Ensure that the relative error in energy norm is small, certainly under 5%, preferably under 1%.
2. Compute the total equivalent strain $\bar{\epsilon}$ in each Gauss point. The elastic equivalent strain is defined as:

$$\bar{\epsilon}^e = \frac{\sqrt{2}}{2(1+\nu)} \sqrt{(\epsilon_1^e - \epsilon_2^e)^2 + (\epsilon_2^e - \epsilon_3^e)^2 + (\epsilon_3^e - \epsilon_1^e)^2} \quad (2)$$

and the plastic equivalent strain is given as:

$$\bar{\epsilon}^p = \frac{\sqrt{2}}{3} \sqrt{(\epsilon_1^p - \epsilon_2^p)^2 + (\epsilon_2^p - \epsilon_3^p)^2 + (\epsilon_3^p - \epsilon_1^p)^2} \quad (3)$$

where ν is Poisson's ratio, $\epsilon_1, \epsilon_2, \epsilon_3$ are the principal strains. The total equivalent strain is:

$$\bar{\epsilon} = \bar{\epsilon}^e + \bar{\epsilon}^p. \quad (4)$$

3. Using $(\bar{\epsilon})^{(k)}$, compute the secant modulus $E_s^{(k)}$ at each Gauss point from the one-dimensional stress-strain curve.
4. In each Gauss point for which $\bar{\epsilon} > \epsilon_Y$ (the uniaxial strain at the onset of yielding), determine the elastic plastic material stiffness matrix using $E_s^{(k)}$. Recompute the stiffness matrices for those elements for which $\bar{\epsilon} > \epsilon_Y$ in one or more Gauss points, and obtain a new finite element solution $u_{FE}^{(k+1)}$.

5. Using $E_s^{(k)}$ and $u_{FE}^{(k+1)}$, compute the strain and stress tensor components and the equivalent stress at each Gauss point. Using expressions (2)-(4), compute the total equivalent strain at each Gauss point $(\bar{\epsilon})^{(k+1)}$. If the equivalent stress $\bar{\sigma}^{(k+1)}$ in each Gauss point satisfies:

$$|\bar{\sigma}_r - \bar{\sigma}^{(k+1)}| \leq \tau |\bar{\sigma}| \quad (5)$$

then stop, else using $(\bar{\epsilon})^{(k+1)}$, compute $E_s^{(k+1)}$, increment k to $k+1$ and return to step 3. In (5), $\bar{\sigma}_r$ is the reference equivalent stress from the uniaxial stress-strain curve corresponding to $(\bar{\epsilon})^{(k+1)}$, and τ is the pre-specified tolerance. The equivalent stress is computed based on the principal stresses as follows:

$$\bar{\sigma} = \frac{\sqrt{2}}{2} \sqrt{(\sigma_1 - \sigma_2)^2 + (\sigma_2 - \sigma_3)^2 + (\sigma_3 - \sigma_1)^2} \quad (6)$$

Fracture Mechanics Parameters

In the neighborhood of the crack tip in an elastic body, the solution becomes singular and the stress values go to infinity at the crack tip. Whether or not a crack will propagate, and at what rate, depends on the energy available to drive crack extension. In linear-elastic fracture mechanics the stress intensity factors are a measure of the stress singularity at the crack tip. They depend on the geometry of the body, the configuration of the crack, the boundary conditions and the loading. In the elastic-plastic regime, the J-integral has been increasingly used to characterize crack initiation and crack growth. J can be interpreted as the energy release rate, and in the linear-elastic case $J=G$ (the energy release rate).

Stress Intensity Factors

The computation of Mode I and II stress intensity factors for linear elastic fracture mechanics was implemented using the Contour Integral Method, as described in ref. 1:

$$K_I = \sqrt{2\pi} A_1^{(1)}, \quad K_{II} = \sqrt{2\pi} A_1^{(2)} \quad (7)$$

where $A_1^{(m)}$, $m = I, 2$, is the first term in the asymptotic expansion of the solution in the neighborhood of the crack tip for modes I and II respectively.

Let Γ_ρ be a circle of radius ρ centered on the crack tip (Figure 3), and assume that ρ is sufficiently close to the crack tip. Then we can write:

$$A_1^{(m)} \approx \int_{\Gamma_\rho} (W^{(m)} T_{FE} - u_{FE} T^W)^{(m)} ds \quad (8)$$

where $W^{(m)}$ is an extraction function, T_{FE} is the traction vector along Γ_ρ computed from the finite element solution u_{FE} , and T^W is the traction vector along Γ_ρ due to the extraction function.

The J-integral

The J-integral provides a mean to determine an energy release rate for cases where plasticity effects are not negligible. In the case of plane stress and plane strain the J-integral is defined by:

$$J = \int_{\Gamma_\rho} (W dy - T \frac{\partial u}{\partial x} ds) \quad (9)$$

where Γ_ρ is a contour around the crack tip, W is the strain energy density:

$$W = W(x, y) = \int_0^\epsilon \sigma_{ij} d\epsilon_{ij}. \quad (10)$$

T is the traction vector (with components T_x, T_y) along Γ_ρ , u is the displacement vector (u_x, u_y) and ds is an element of Γ_ρ . The coordinate system is located such that the origin is in the crack tip, the x-direction is parallel to the crack face (see Figure 3).

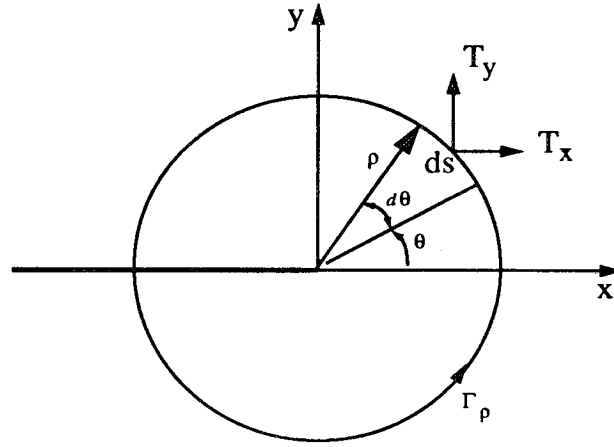


Figure 3. Path around the crack tip.

If the integration is performed along a circular path of radius ρ centered at the crack tip, equation (9) can be written as:

$$J = \int_{-\pi}^{\pi} (W \cos \theta - T_x \frac{\partial u_x}{\partial x} - T_y \frac{\partial u_y}{\partial x}) \rho d\theta. \quad (11)$$

The J-integral can be computed for linear and nonlinear isotropic or orthotropic materials. For the case of elastic-plastic materials, the integration path should be selected in such a way that it does not cut through the plastic zone around the crack tip. In the plastic region the strain energy density (W) is not defined.

EXAMPLE PROBLEM

Problem Description

The model problem consists of a 2024-T3 aluminum alloy plate with six equally spaced holes and a crack emanating from each hole. The cracks are of different sizes and the panel is subjected to a remote tensile load. The panel was selected from ref. 3, and corresponds to an MSD test coupon for constant ampli-

tude crack growth testing. Numerical and experimental crack growth data are available for the panel. Figure 4 shows the configuration of the panel for the example problem.

The objective of the analysis is to compute the stress intensity factors and the J-integral for each crack at different stages during crack propagation. The results are compared with the experimental values. The elastic-plastic analysis is performed using two different stress-strain laws: Ramberg-Osgood and elastic-ideally-plastic. The length of each crack (measured from the edge of the hole) for the four cases analyzed is

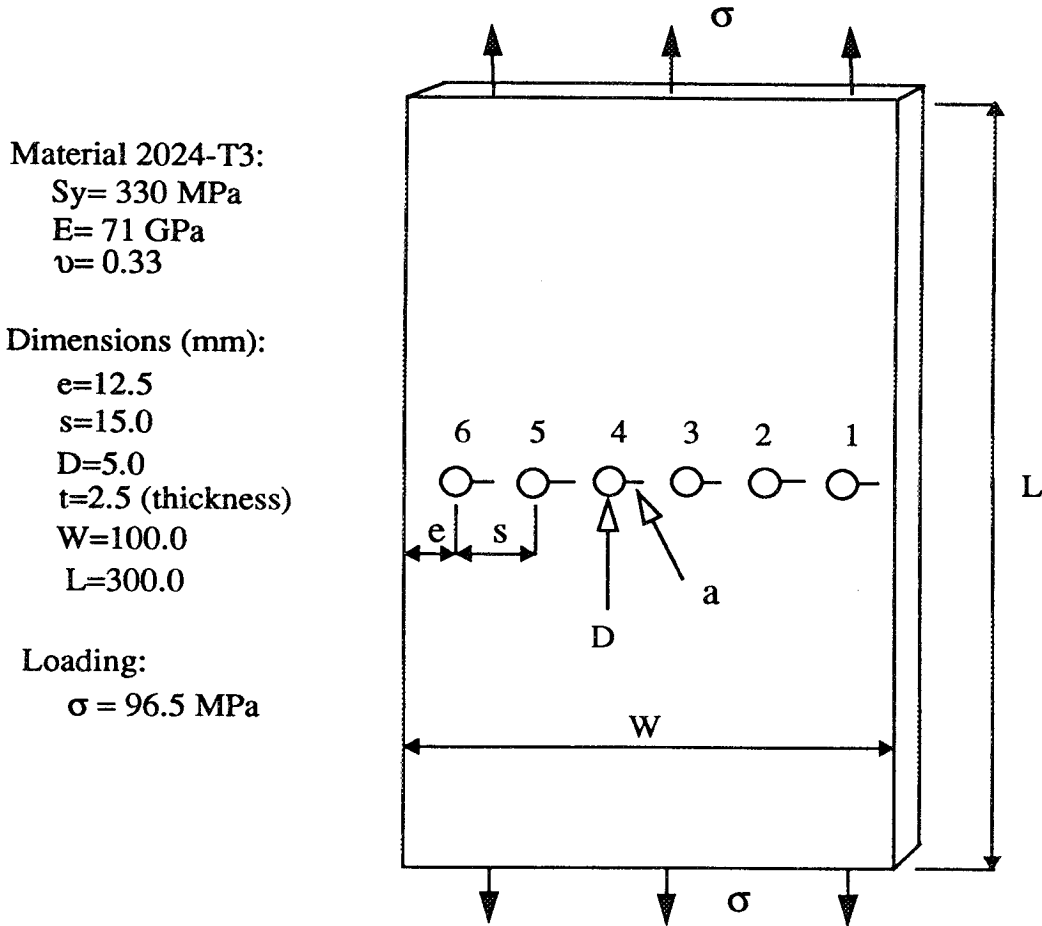


Figure 4. Panel configuration for example problem.

shown in Table 1. Case 1 corresponds to the initial crack length values; Case 2 represents the crack lengths after 6000 loading cycles; Case 3 after 12000 cycles; and Case 4 represents the crack lengths at failure (~13500 cycles).

Table 1: Crack Length (mm) for Each Case

Case	a_1	a_2	a_3	a_4	a_5	a_6
1	3.00	2.08	2.38	2.47	2.00	2.03
2	4.35	3.48	3.70	3.70	3.26	3.26
3	6.74	5.87	6.09	5.87	5.09	4.78
4	7.78	7.90	7.90	6.89	5.78	5.11

Discretization

In designing the finite element mesh and selecting the other discretization parameters, the smoothness of the exact solution of the mathematical model representing the physical system should be considered. For the example problem, the following modeling aspects are relevant:

1. Two-dimensional (plane stress) analysis is considered appropriate for this case.
2. Due to symmetry conditions, only half of the panel needs to be analyzed.
3. Elastic-plastic material properties are used to assess the influence of crack tip plasticity on the fracture mechanics parameters.

The solution of the mathematical model just described is smooth inside the domain and on the boundaries, except at the crack tips where the stresses are unbounded in the linear case. For the nonlinear case when the material is elastic-perfectly plastic, the stresses are finite but the strains are singular at the crack tips. The design of the finite element mesh should account for the nature of the exact solution. Geometrically graded meshes toward the singular points are known to be optimal in conjunction with p-extension for problems of this type. However, the design of geometrically graded meshes for domains with multiple cracks emanating from holes with sizes comparable to the hole diameters is very cumbersome and in many cases impractical. For that reason, the use of very simple meshes combined with high order elements (product space) is selected. This strategy has been tested and documented in refs. 3 and 4.

The finite element mesh consisting of 38 quadrilateral elements is shown in Figure 5. Each crack has been defined parametrically, so that the same mesh could be used for the four cases shown in Table 1 by adjusting the crack length parameters. Note that no mesh refinement around the crack tips has been used. Due to symmetry, only half the panel was discretized.

Two elastic-plastic stress-strain relations were investigated. The Ramberg-Osgood material characterized by: $E=71$ GPa, $\nu=0.33$, $S_{70E}=320$ MPa, $n=12$, and the elastic-perfectly plastic material characterized by $S_y=330$ MPa. The linear solution was computed for the product space and polynomial degree ranging from 1 to 8. Four nonlinear solutions were computed for each case in order to obtain an assessment of the discretization error for the nonlinear analysis. The linear runs corresponding to p-levels 5, 6, 7 and 8 were used to start the nonlinear iterations. The number of iterations required to complete any given analysis was based on a specified tolerance of 1.0% (see Eq. 5).

Results

Discretization Errors

For each linear analysis, the estimated relative error in energy norm was computed from the eight available solutions. Table 2 shows a typical result which corresponds to Case 1. The reported rate of convergence is typical for the p-extension in the case of category B type problems without geometrically graded meshes towards the singular points. For cases 1, 2 and 3, the estimated relative error in energy norm corresponding to p-level=5 and above was less than 5%.

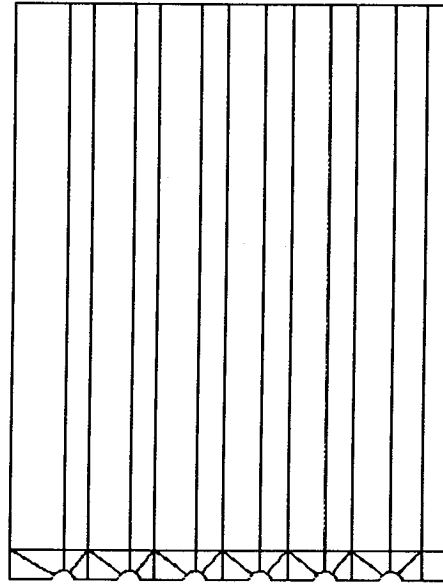


Figure 5. Finite element mesh.

Table 2: Estimated Relative Error in Energy Norm. Linear Solution for Case 1

p-Level	DOF	Potential Energy [N mm]	Rate of Convergence	Estimated % Error
1	117	-2490.4413	0.00	10.23
2	392	-2504.4379	0.31	7.02
3	819	-2510.8236	0.50	4.86
4	1398	-2513.3046	0.51	3.71
5	2129	-2514.6060	0.56	2.93
6	3012	-2515.3562	0.62	2.37
7	4047	-2515.7996	0.64	1.96
8	5234	-2516.0703	0.64	1.66

The fracture mechanics parameters were computed for the available sequence of linear and nonlinear solutions: Eight runs for each linear case and 4 runs for each nonlinear case. Convergence of the extracted results was assessed in each case. Typical convergence data are shown in Table 3 for the linear and nonlinear fracture mechanics parameters of Case 2, Crack 1.

Fracture Mechanics Parameters

Tables 4 to 6 show the values of the fracture mechanics parameters (FMP) for each crack and for cases 1 to 3 respectively. They include the stress intensity factor (K_I), the J-integral (J_e) computed from the linear solution and the values of the J-integral computed from the elastic-plastic solution for the Ramberg-Osgood material (J_p^{RO}) and the elastic-perfectly plastic material (J_p^{EP}). The relative difference between the elastic

and plastic (Ramberg-Osgood) values of J is also included. All values included in the tables correspond to the linear or nonlinear solutions for p -level=8.

Table 3: Convergence Data for Case 2, Crack 1

p-Level	K_I [MPa m ^{1/2}]	J_e [N m ⁻¹]	J_p^{RO} [N m ⁻¹]	J_p^{EP} [N m ⁻¹]
1	11.26	1148	---	---
2	14.43	2567	---	---
3	13.84	2647	---	---
4	13.41	2531	---	---
5	13.90	2681	2737	2683
6	14.28	2822	2881	2825
7	14.22	2827	2925	2859
8	14.15	2815	2927	2864

Table 4: FMP for Case 1 (N=0)

Parameter	Value of the Parameter for Crack #					
	1	2	3	4	5	6
K_I [MPa m ^{1/2}]	12.65	12.40	12.49	12.49	12.11	11.95
J_e [N m ⁻¹]	2242	2151	2186	2185	2059	2000
J_p^{RO} [N m ⁻¹]	2276	2200	2236	2231	2097	2031
J_p^{EP} [N m ⁻¹]	2256	2176	2219	2218	2084	2015
$(J_p^{RO}-J_e)/J_e$ [%]	1.8	2.3	2.3	1.8	1.9	1.5

Table 5: FMP for Case 2 (N=6000)

Parameter	Value of the Parameter for Crack #					
	1	2	3	4	5	6
K_I [MPa m ^{1/2}]	14.15	14.20	14.17	14.04	13.62	13.24
J_e [N m ⁻¹]	2815	2817	2818	2769	2592	2448
J_p^{RO} [N m ⁻¹]	2927	2905	2900	2843	2653	2491
J_p^{EP} [N m ⁻¹]	2864	2840	2837	2785	2609	2458
$(J_p^{RO}-J_e)/J_e$ [%]	4.3	3.3	2.8	2.5	2.3	1.6

Table 6: FMP for Case 3 (N=12000)

Parameter	Value of the Parameter for Crack #					
	1	2	3	4	5	6
K_I [MPa m ^{1/2}]	18.78	19.26	19.04	18.21	16.67	15.39
J_e [N m ⁻¹]	4885	5152	5019	4604	3893	3325
J_p^{RO} [N m ⁻¹]	6292	7057	6681	5786	4504	3603
J_p^{EP} [N m ⁻¹]	5585	6072	5771	5151	4196	3497
$(J_p^{RO}-J_e)/J_e$ [%]	28.6	37.1	33.1	25.9	15.7	8.1

These results clearly indicate that the stress intensity factors are not substantially affected by crack tip plasticity until the number of cycles is sufficiently high (near the end of the life of the panel). This is in agreement with the experimental observation: Towards the end of the life, the actual fatigue crack propagation rate is larger than that predicted by using the linear stress intensity factors. Tables 7 to 9 show a comparison of the experimental crack propagation rate (ref. 3) with those computed from the expression:

$$\frac{da}{dN} = C (\Delta K)^m \quad (12)$$

for the linear solution and from the expression:

$$\frac{da}{dN} = C (\sqrt{E \cdot \Delta J_p})^m \quad (13)$$

for the nonlinear solution. C and m are material constants ($C=4.15 \times 10^{-8}$, $m=2.2$ when ΔK is given in ksi, and da/dN is given in inch/cycle). The values of J_p for the Ramberg-Osgood (R-O) and for the elastic-perfectly-plastic material (E-P) are considered in Eq. 13.

Table 7: Fatigue Crack Propagation Rates for Case 1 (N=0)

Propagation Rate given by	da/dN [10 ⁴ mm/cycle] for Crack #					
	1	2	3	4	5	6
Eq. 12	2.28	2.18	2.21	2.21	2.07	2.01
Eq. 13(R-O)	2.30	2.21	2.25	2.25	2.10	2.03
Eq. 13 (E-P)	2.28	2.19	2.23	2.23	2.09	2.01
Experimental	2.10	2.20	2.16	2.00	1.75	1.80

Table 8: Fatigue Crack Propagation Rates for Case 2 (N=6000)

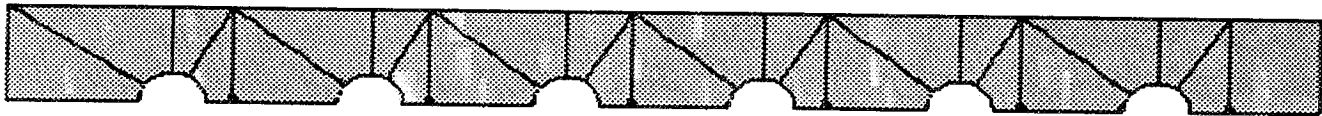
Propagation Rate given by	da/dN [10^{-4} mm/cycle] for Crack #					
	a ₁	a ₂	a ₃	a ₄	a ₅	a ₆
Eq. 12	2.92	2.93	2.92	2.86	2.68	2.49
Eq. 13(R-O)	3.03	3.01	3.00	2.94	2.72	2.54
Eq.13 (E-P)	2.96	2.93	2.93	2.87	2.69	2.50
Experimental	2.91	2.69	2.92	2.64	2.52	2.20

Table 9: Fatigue Crack Propagation Rates for Case 3 (N=12000)

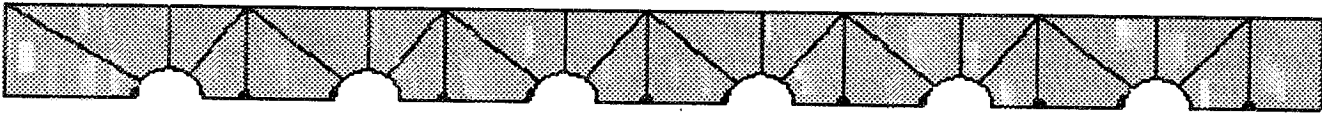
Propagation Rate given by	da/dN [10^{-4} mm/cycle] for Crack #					
	a ₁	a ₂	a ₃	a ₄	a ₅	a ₆
Eq. 12	5.43	5.74	5.60	5.08	4.18	3.49
Eq. 13 (R-O)	7.03	7.98	7.51	6.41	4.87	3.81
Eq. 13 (E-P)	6.17	6.76	6.40	5.64	4.50	3.69
Experimental	7.12	8.95	7.56	6.40	5.30	3.47

The Plastic Zone Size

Figure 6 shows the extent of the plastic zone at each crack tip for cases 1, 2 and 3 for the Ramberg-Osgood stress-strain law. The plastic zone is the set of all points for which the total equivalent strain is greater than or equal to the uniaxial yield strain $\bar{\epsilon} \geq \epsilon_Y$, where $\epsilon_Y = S_Y/E$.



Case 1: N=0



Case 2: N=6000



Case 3: N=12000

Figure 6. Plastic zone sizes for Ramberg-Osgood material.

Limit Load

The limit load was computed for the elastic-perfectly plastic material, by imposing a uniform normal displacement along the top edge of the panel, and computing the stress resultant along that edge. The crack configuration of Case 4 (failure condition) was used, and a nonlinear solution was obtained for each value of the imposed displacement. The results are shown in Figure 7. The limit load for this problem can be estimated as:

$$P_L = S_Y \left(W - 6d - \sum_{i=1}^6 a_i \right) t = 330 (100 - 30 - 41.36) 2.5 = 23628 \text{ N}$$

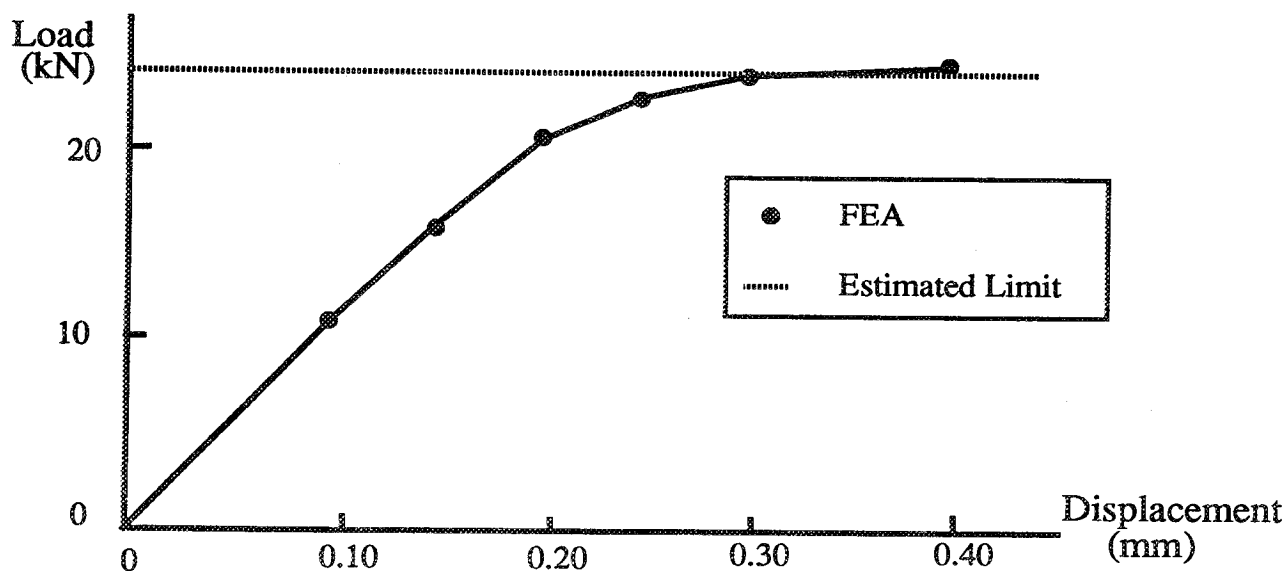


Figure 7: Load-displacement relation for case 4, elastic-perfectly plastic material.

Time Requirements

One important consideration in the utilization of an analysis tool incorporating advanced methodology is the amount of time required to analyze a problem of substantial complexity like the one discussed in this paper. To address this issue, we report in this Section the amount of time spent in the linear and nonlinear analyses. The computer runs were performed on a HP 9000/715 workstation using the finite element code STRESS CHECK¹ developed by the authors. The total time is the sum of the time required to perform three main activities: (1) preparation of input data, (2) execution of analyses, and (3) extraction of results.

The preparation of input data consists of the description of the solution domain, the design of the finite element mesh, the specification of the material properties, and the assignment of the boundary conditions (loads and constraints). This involves almost exclusively engineering time which will depend on the level of training of the analyst, and on the characteristics of the software tool used. The preparation of input data for the problem shown in Figure 5 required approximately 20 minutes of wall clock time. Since the crack

1. STRESS CHECK is a trademark of Engineering Software Research and Development, Inc., 7750 Clayton Rd., Suite 204, St. Louis, MO 63117.

lengths were defined in parametric form, and since the same description can be used to perform linear and nonlinear analyses, only one mesh was used for all cases analyzed.

The execution time depends on the analysis type. To obtain a sequence of linear solutions (p-level=1 to 8), 1.5 minutes of CPU time were required for each case. For the nonlinear solutions, the CPU time depends on the number of iterations necessary to achieve the desired tolerance level (see Eq. 5), which in turn depends on the amount of plasticity associated with the solution. To obtain a sequence of nonlinear solutions (p-level=5 to 8) for the crack configuration of case 1, 9.5 minutes of CPU were required; for case 2, 10.4 minutes of CPU; for case 3, 18.0 minutes of CPU.

The extraction of the results (the fracture mechanics parameters) involves mostly analyst's time. To compute the six crack tip stress intensity factors and J-integral (both elastic and plastic) for each case analyzed, about 30 minutes of wall clock time were required.

In summary, a complete analysis of a multiple-site damage panel for one crack configuration, including preparation of input data, execution of a sequence of linear and nonlinear solutions, and extraction of the data of interest, can be performed in about 1.5 hours of wall clock time.

The Importance of Controlling Discretization Errors

Intrinsic control of discretization errors by finite element programs is very important for properly correlating computed information with experimentally observed data and for using computed data in engineering decisions which cannot be measured directly, and/or exploring a range of loadings and constraint conditions, not covered by the experiment.

To illustrate this point, let Φ_{EXP} be some experimental information, for example a measured displacement or strain, Φ_{MOD} the same information predicted by a mathematical model, for example the equations of elasticity together with the appropriate material properties, boundary conditions and loading data; Φ_{FEA} the same information predicted by a finite element approximation of the mathematical model. Φ_{MOD} is generally not known, nevertheless the purpose of an experiment is to determine whether the mathematical model correctly describes the physical system being modeled, that is, whether Φ_{MOD} is sufficiently close to Φ_{EXP} . Writing:

$$|\Phi_{EXP} - \Phi_{MOD}| \equiv |\Phi_{EXP} - \Phi_{FEA} + \Phi_{FEA} - \Phi_{MOD}| \leq |\Phi_{EXP} - \Phi_{FEA}| + |\Phi_{FEA} - \Phi_{MOD}| \quad (14)$$

it is seen that if the quality of a mathematical model is to be assured then it is necessary to ensure that $|\Phi_{FEA} - \Phi_{MOD}|$ is not larger, and preferably much smaller, than $|\Phi_{EXP} - \Phi_{FEA}|$, which is known from measurement and computation. The quality control procedures of any finite element program should make it possible to ascertain that $|\Phi_{FEA} - \Phi_{MOD}|$ is smaller than $|\Phi_{EXP} - \Phi_{FEA}|$.

Unfortunately, there are many examples in industrial practice where close correlation with experimental results is achieved through skillful manipulation of the discretization parameters. The sensitivity of the approximate solution to discretization parameters is a strong indication that the numerical error is large, or the model is improperly defined. In the absence of intrinsic procedures designed for controlling approximation errors, it is possible to correlate computed data with experimental observations through near cancellation of two large errors:

$$\Phi_{EXP} - \Phi_{FEA} \equiv \underbrace{\Phi_{EXP} - \Phi_{MOD}}_{\pm M} + \underbrace{\Phi_{MOD} - \Phi_{FEA}}_{\pm M} \approx 0 \quad (15)$$

where M is some big number. Such models are unreliable and can be very misleading when the model is used for drawing general conclusions from experimental information.

CONCLUSIONS

Control of errors of discretization and modeling can be achieved if the analysis tools provide sufficient flexibility and are easy to use. It is also required that complex problems, both linear and nonlinear, be solved in hours instead of days.

Advanced analysis methods for the computation of stress intensity factors and the J-integral under conditions of small scale plasticity have been implemented within the framework of the p-version of the finite element method. The implementation makes it possible for practicing engineers to assess damage in structural components under elastic-plastic conditions with guaranteed reliability. The key elements which make this implementation unique can be summarized as follows:

1. The use of the product space and superconvergent extraction for the stress intensity factors allows the use of very simple (coarse) meshes to obtain extremely reliable results for the linear elastic fracture mechanics parameters.
2. The use of the deformation theory of plasticity with the von Mises yield criterion and the high-order finite elements (product space) makes it possible to use the same coarse meshes for the elastic-plastic analysis. Plastic zone sizes, J-integrals and limit loads can be easily and reliably computed from the finite element solutions.
3. The availability of various representations for nonlinear material makes it possible to assess the influence of different stress-strain laws in the results.
4. The possibility of using spring boundary conditions, bearing loads, and precise geometric representations allows for closer representation of actual problems.

The application of these techniques to a multi-site damage panel clearly demonstrates that the investigation of different modeling assumptions can be accomplished in a reasonable amount of time, and that the results obtained can be used to assess the influence of plasticity on the residual strength of the panel.

REFERENCES

1. Szabo, B. A.; and Babuska, I.: *Finite Element Analysis*. John Willey and Sons, Inc., 1991.
2. Szabo, B. A.; Actis, R. L.; and Holzer, S. M.: Solution of Elastic-Plastic Stress Analysis Problems by the p-Version of the Finite Element Method. Center for Computational Mechanics, Washington University, St. Louis, MO 63130, Report WU/CCM-93/3, November 1993.
3. Nathan, A.; and Brot, A.: An Analytical Approach to Multi-Site Damage. 17th Symposium of the International Committee on Aeronautical Fatigue, Stockholm, Sweden, June 10, 1993.
4. Actis, R. L.; and Szabo, B. A.: Computation of Stress Intensity Factors for Panels with Multi-Site Damage. Center for Computational Mechanics, Washington University, St. Louis, MO 63130, Technical Note WU/CCM-92/3, December 1992.